Volume 5, Issue 8, August 2015 ISSN: 2277 128X

International Journal of Advanced Research in Computer Science and Software Engineering

Research Paper

Available online at: www.ijarcsse.com

Wavelet Transform of Block Based Polynomial Coding for Image Compression

Dr. Ghadah Al-Khafaji
Dept. of Computer Science,
Baghdad University, Iraq

Haider Al-Mahmood
Dept. of Computer Science,
Al-Mustansiriyah University, Iraq

Abstract: This paper proposed a hybrid compression system that utilized both the frequency and spatial domains efficiently using the discrete wavelet transform of block based along with the polynomial coding. The test results showed the potential integrity of the proposed technique of high efficiency in terms of compression ratio and quality.

Key words: Image compression, wavelet transform, block based, polynomial prediction coding.

I. INTRODUCTION

Image compression can be recognized as an enabling technology that looks like art of science that becomes urgently needed with the immense revolution in computers, smart phones and communication.

People daily communicate and convey information easily through images using phones and computers that characterized by the limited memory size and communication band width, so compression process successfully reducing the data amount required to increase the phones/computers and communication efficiency.

Image compression basically based on removing the observed and/or unobserved redundancies between the embedded observed pixels (i.e., interpixel redundancy), the unobserved of representation of pixel values using the fixed length binary coded (i.e., coding redundancy) and the unobserved of human visual system (i.e., psychovisual redundancy), where the techniques simply classified into lossless and lossy depending on the redundancy(s) way exploited, more details can be found in [1-6].

Today, there is a continuous commercial demand on construction of standards image compression techniques that vary according to their requirements to meet its need for natural images, medical images and text images, various available standards can be found in [7-11].

In general, these standards techniques based on the hybrid compression system base that efficiently utilized the mixing between the spatial domain and frequency domain.

In this paper, the discrete wavelet transform (DWT) of block based of frequency domain along with the polynomial coding of linear approximation modelling of spatial domain exploited effectively to compress natural images, where the proposed techniques discussed in section 2 followed by the experimental results in section 3.

II. THE PROPOSED HYBRID COMPRESSION SYSTEM

Figure (1) shows the structure of the suggested compression system that makes use of both the spatial and frequency domains to increase the system performance by tacking advantages of mixed between the techniques of different domain base. The following steps below illustrated the proposed system clearly:

1- The input to the compression system corresponds to the uncompressed image I of size $N{\times}N$ of huge redundancies embedded.

2-Partition the image I into fixed blocks of sizes $n{\times}n$ (i.e., $8{\times}8$ or $16{\times}16$) to exploited the partial correlation or the local dependency between neighbouring pixels (interpixel redundancy).

3- For each fixed partitioned block resultant from step above, apply two level discrete wavelet transform (DWT) decomposition, in other words, the first layer decompose each block into approximation and detail sub bands ($LowLow_1$, $LowHigh_1$, $HighLow_1$ and $HighHigh_1$) of size ($N/2{\times}N/2$) (i.e., $4{\times}4$ or $8{\times}8$), then the second layer decompose the approximation sub-band ($LowLow_1$) into approximation and detail sub bands ($LowLow_2$, $LowHigh_2$, $HighLow_2$ and $HighHigh_2$) each of size ($N/4{\times}N/4$) (i.e., $2{\times}2$ or $4{\times}4$). In this step the interpixel (spatial) redundancy removed to decorrelate the embedded observed redundancy [12].

$$LH_1Q = round(\frac{LH_1}{QL_1}) \rightarrow LH_1D = LH_1Q \times QL_1 \text{.............}(1)$$

$$HL_1Q = round(\frac{HL_1}{QL_1}) \rightarrow HL_1D = HL_1Q \times QL_1 \text{.............}(2)$$

$$HH_1Q = round(\frac{HH_1}{QL_1}) \rightarrow HH_1D = HH_1Q \times QL_1 \text{.............}(3)$$

$$LH_2Q = round(\frac{LH_2}{QL_2}) \rightarrow LH_2D = LH_2Q \times QL_2 \text{.............}(4)$$

$$HL_2Q = round(\frac{HL_2}{QL_2}) \rightarrow HL_2D = HL_2Q \times QL_2 \text{.............}(5)$$

$$HH_2Q = round(\frac{HH_2}{QL_2}) \rightarrow HH_2D = HH_2Q \times QL_2 \text{.............}(6)$$

4- Use the scalar uniform quantizer to remove the unobserved psychovisual redundancy of the details sub bands of the first and second layer according to equations (1-6).

Where LH_1Q, HL_1Q, HH_1Q, LH_2Q, HL_2Q, HH_2Q and LH_1D, HL_1D, HH_1D, LH_2D, HL_2D, HH_2D are the quantized/dequantized sub bands of $layer_1$ and $layer_2$ respectively of two quantization steps for the first and second layer details sub bands.

5- The approximation subband of $layer_2$ (LL_2), utilized the polynomial coding of linear approximation base (first order Taylor series form) that implicitly composed of the following sub steps:

a- Compute the coefficients of linear polynomial coding base using the following equations (7-9) [13].

$$a_0 = \frac{1}{n\times n}\sum_{i=0}^{n/4-1}\sum_{j=0}^{n/4-1} LL_2(i,j) \quad \text{.............(7)}$$

$$a_1 = \frac{\sum_{i=0}^{n/4-1}\sum_{j=0}^{n/4-1} LL_2(i,j)\times(j-x_c)}{\sum_{i=0}^{n/4-1}\sum_{j=0}^{n/4-1}(j-x_c)^2} \quad \text{.......(8)}$$

$$a_2 = \frac{\sum_{i=0}^{n/4-1}\sum_{j=0}^{n/4-1} LL_2(i,j)\times(i-y_c)}{\sum_{i=0}^{n/4-1}\sum_{j=0}^{n/4-1}(i-y_c)^2} \quad \text{.......(9)}$$

b- Remove the psychovisual redundancy embedded between the computed coefficients above using the scalar uniform quantizer.

$$a_0Q = round\left(\frac{a_0}{QS_{a0}}\right) \rightarrow a_0D = a_0Q \times QS_{a0} \quad \text{........(10)}$$

$$a_1Q = round\left(\frac{a_1}{QS_{a1}}\right) \rightarrow a_1D = a_1Q \times QS_{a1} \quad \text{..........(11)}$$

$$a_2Q = round\left(\frac{a_2}{QS_{a1}}\right) \rightarrow a_2D = a_2Q \times QS_{a1} \quad \text{........(12)}$$

Where a_0Q, a_1Q, a_2Q and a_0D, a_1D, a_2D are the polynomial quantized/dequantized coefficients respectively of two quantization steps QS_{a0},QS_{a1}.

c- Create the approximated image $\tilde{LL}_2$ that resemble the original approximated sub band.

$$\tilde{LL}_2 = a_0D + a_1D(j-x_c) + a_2D(i-y_c) \quad \text{.....(13)}$$

d- Find the residual or residue between the between the original LL_2 and the predicted one $\tilde{LL}_2$.

$$R(i,j) = LL_2(i,j) - \tilde{LL}_2(i,j) \quad \text{.......................................(14)}$$

e- Remove the psychovisual redundancy of residual image using the same process of scalar uniform quantizer

$$RQ = round\left(\frac{R}{QS_R}\right) \rightarrow RD = RQ \times QS_R \quad \text{........(15)}$$

6- To remove the unobserved redundancy of representation binary coded number (coding redundancy) use Huffman coding to the quantized detail sub bands of the two layers and the quantized coefficients, while the LZW use for the residual image. Theses coded information corresponds to the compressed information that actually filtered out of the redundancies as much as possible.

7- The decoder reconstructs the compressed image, by firstly utilizing the decoded information of dequantized polynomial coefficients and residual to reconstruct the approximation subband (LL_2) of $layer_2$ of each block, that hierarchally used with the $layer_2$ sub bands to reconstruct the first layer approximation subband that exploited to rebuilt the compressed image $\hat{I}$

$$\hat{LL}_2(i,j) = RD(i,j) + \tilde{LL}_2(i,j) \quad \text{........(16)}$$

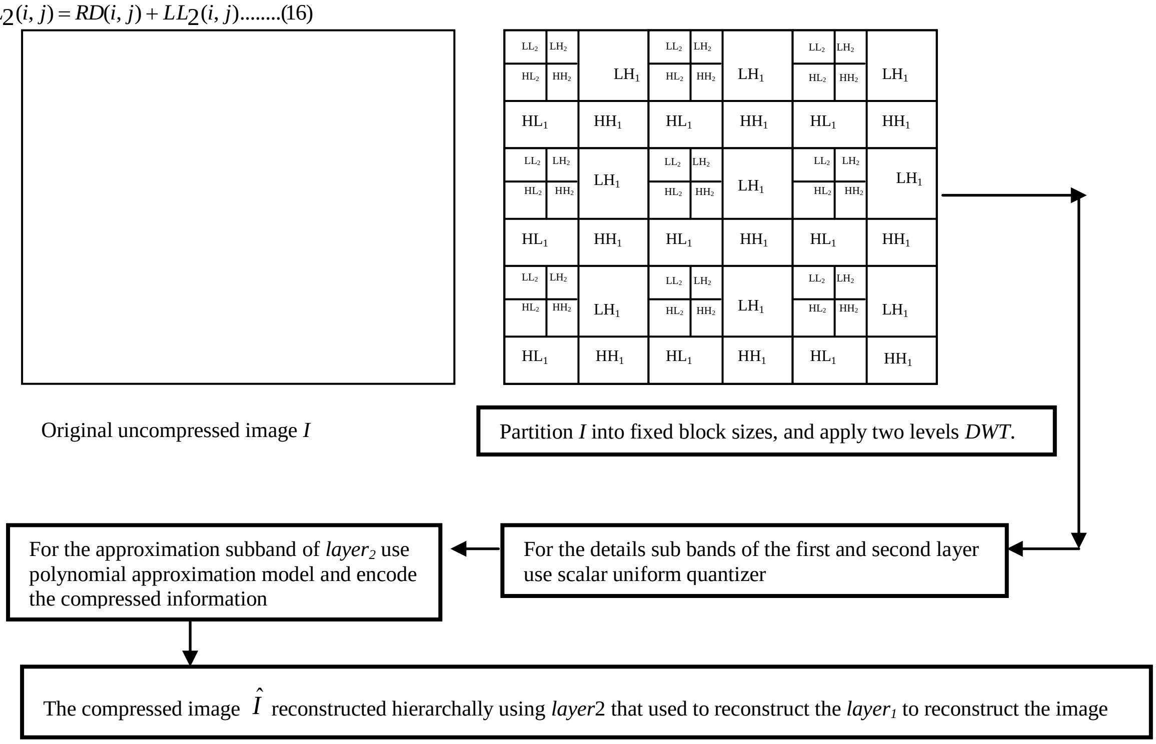

Fig. (1): The proposed compression system structure.

III. EXPERIMENTS and RESULTS

To evaluate the performance of the proposed compression system, using the objective fidelity criteria of the Peak Signal to Noise Ratio (PSNR) corresponding to measure of goodness between original image I and the compressed image $\hat{I}$ (see equation 17) along with the compression ratio corresponding to measure of efficiency that defined as the ratio size of both the original image information to the compressed image information

$$PSNR = 10.\log_{10}\left[\frac{(255)^2}{\frac{1}{N\times N}\sum_{x=0}^{N-1}\sum_{y=0}^{N-1}\left[(\hat{I}(x,y)-I(x,y)\right]^2}\right] \quad ....(17)$$

Three tested standard images adopted as shown in figure (2), where all the images are square of size 256×256 pixels of 8 bit/per pixel (i.e., gray scale images), also used one quantization level values of all details subband of each layer (i.e., one quantization level to *layer*$_1$ details sub bands (*LowHigh*$_1$, *HighLow*$_1$ and *HighHigh*$_1$) and another quantization step for *layer*$_2$ details sub bands (*LowHigh*$_2$, *HighLow*$_2$ and *HighHigh*$_2$)), and quantization step of coefficients are equal to 1,1,1 and quantization step for residual either 5 or 25.

Fig. (2): Three tested standard images (a) Lena, (b) Cameraman, (c) Rose, all images of square of size 256×256, gray scale images.

The results shown in table (1) using quantization level of *layer*$_2$ is twice than the quantization level of layer1 of details sub bands. Obviously, that the technique utilized the wavelet transform of each block of multiresolution base provides efficient performance due to preserves the image information hierarchally. The essential use of the combination between the frequency and spatial domains, leads to small effects of spatial domain where the technique unaffected by the image details. Namely, if the polynomial coding of spatial domain adopted only, the results greatly affected by the image details, while here less effects due to combination of the domains. Also, the results imply smaller performance changes for different quantization residual level values (i.e., 5 and 25) because of the small size of the residual image (i.e., small amount of information). Lastly, it is clear that the quantization levels affected both the quality and the compression ratio, different quantization levels values meaning either decrease/ increase the quality/compression ratio. Figure (3) illustrates the compressed image quality of the tested images using different quantization level values.

Table (1): The performance of the proposed compression system, using block size of 8×8 and different quantization level values.

Tested images	**Quantization level of *Layer*$_1$ details sub bands (*LH*$_1$,*HL*$_1$ & *HH*$_1$)**	**Quantization level of *Layer*$_2$ details sub bands (*LH*$_2$,*HL*$_2$ & *HH*$_2$)**	**Quantization level of polynomial coefficients (1,1,1) with Quantization Step of Residual**	**Compression Ratio**	**PSNR**
Lena	4	8	5	17.8816	27.1805
	4	8	25	22.6377	27.1737
	8	16	5	12.3234	31.2777
	8	16	25	14.4099	31.2602
	16	32	5	8.3945	35.5952
	16	32	25	9.3131	35.5480
	32	64	5	5.8462	40.8912
	32	64	25	6.2774	40.7335
Cameraman	4	8	5	20.7919	27.2800
	4	8	25	24.5269	27.2732
	8	16	5	14.5023	31.7098
	8	16	25	16.2258	31.6909
	16	32	5	10.4108	36.4507
	16	32	25	11.2702	36.3945
	32	64	5	7.7443	41.1854

	32	64	25	8.2156	41.0206
Rose	4	8	5	19.7160	29.0399
	4	8	25	25.4213	29.0296
	8	16	5	13.5042	32.8957
	8	16	25	15.9571	32.8726
	16	32	5	9.0084	37.5138
	16	32	25	10.0377	37.4422
	32	64	5	6.4113	42.8428
	32	64	25	6.9160	42.6033

Quantization levels of $layer_1$=4, $layer_2$=8 Residual=5	Quantization levels of $layer_1$=8, $layer_2$=16 Residual=5	Quantization levels of $layer_1$=16, $layer_2$=32 Residual=5	Quantization levels of $layer_1$=32, $layer_2$=64 Residual=5
 CR= 17.8816 PSNR= 27.1805	 CR=12.3234 PSNR=31.2777	 CR=8.3945 PSNR=35.5952	 CR=5.8462 PSNR=40.8912
 CR=20.7919 PSNR=27.2800	 CR=14.5023 PSNR=31.7098	 CR=10.4108 PSNR=36.4507	 CR=7.7443 PSNR=41.1854
 CR=19.7160 PSNR=29.0399	 CR=13.5042 PSNR=32.8957	 CR=9.0084 PSNR=37.5138	 CR=6.4113 PSNR=42.8428

Fig. (3): Compressed tested images with different quality and compression ratios.

IV. CONCLUSIONS

The results shown in this paper leads to high efficiency due to integrity of both the hybrid compression techniques along with the black based scheme.

REFERENCES

[1] Maneesha, G., Amit K. and Abhishek, K. 2011. Review: Image Compression Algorithm. International Journal of Computer Science & Engineering Technology, 1(10), 649-654.

[2] Padmaja, V. and Chandrasekhar, B. 2012. Literature Review of Image Compression Algorithm. International Journal of Scientific & Engineering Research, 3(6), 1-6.

[3] Asha, L. and Permender, S. 2013. Review of Image Compression Techniques. International Journal of Emerging Technology and Advanced Engineering, 3(7),461-464.

[4] Kitty, A. and Manshi, S. 2014. A Comprehensive Review of Image Compression Techniques. International Journal of Computer Science and Information Technologies, 5(2), 1169-1172.

[5] Pratishtha, G., Purohit, G. and Varsha, B. 2014. A Survey on Image Compression Techniques. International Journal of Advanced Research in Computer and Communication Engineering, 3(8),7762-7768.

[6] Priya, K., Sunaina, K. and Gurpreet, K. 2014. A Review of Image Compression. International Journal of Advanced Research in Computer Science and Software Enginnering, 4(9), 128-132.

[7] Ghanbari, M. 1999. Video Coding an Introduction to Standard Codecs. Institution of Electrical Engineers, London.
[8] Christopoulos, C., Skodras, A. and Ebrahimi, T. 2000. The JPEG2000 Still Image XOSING System: an Overview. IEEE Transactions on Consumer Electronics, 46(4), 1103-1127.
[9] Ghanbari, M. 2003. Standard Codecs: Image Compression to Advanced Video Coding. Institution of Electrical Engineers, London.
[10] Gonzalez, R. C. and Woods, R. E. 2003. Digital Image Processing 2nd edn. Prentice Hall.
[11] Grigorios D. , Zervas N., Sklavos N. and Costas E. 2008. Design Techniques and Implementation of Low Power High-Throughput Discrete Wavelet Transform Tilters for JPEG 2000 Standard. WASET , International Journal of Signal Processing 4(1), 36-43.
[12] Mohammed, M. and Ghadah, Al-K. 2013. Applied Minimized Matrix Size Algorithm on the Transformed Images by DCT and DWT used for Image Compression. International Journal of Computer Applications, 70(15), 33-40.
[13] Ghadah, Al-K. and Haider, Al-M. 2013. Lossless Compression of Medical Images using Multiresolution Polynomial Approximation Model. International Journal of Computer Applications, 76(3),38-42.

